PROCESS AND DEVICE MODELING
W.L. Engl (Editor)
© Elsevier Science Publishers B.V. (North-Holland), 1986

Chapter 8

ON MODELING MOS-DEVICES

Siegfried SELBERHERR

Institut für Allgemeine Elektrotechnik und Elektronik
Abteilung für Computerunterstütztes Konstruieren
Technische Universität Wien, Vienna, Austria

The topic of modern MOS-Transistor modeling is reviewed. Models for surface scattering and impact ionization, physical parameters which are of particular relevance for MOS-Transistor simulation programs, are explained. Guidelines to a mathematical analysis of the fundamental equations, which allow the judgement of numerical methods for their applicability, are presented. Examples of applications of simulation programs on the analysis of problems which are important at present are sketched.

INTRODUCTION

Since 1960 when the demonstration of the practically usable MOS-Transistor took place [41], it's development has shown to evolve dramatically. Today, 25 years later, integrated circuits with more than 400.000 devices per single chip are manufactured. In order to minimize the number of cycles of trial and error in device fabrication improved understanding of basic device operation has attained crucial importance. Thus, numerical modeling of MOS-Transistors has become a basic requirement for the development of prototype devices. although the first modeling attempts were made relatively recently. A two dimensional solution of Poisson's equation with application to a MOS structure was probably first published by Loeb et al. [48] and Schroeder and Muller [74] in 1968. Since then a lot of work has been contributed dealing with simulation of MOS devices due to their intrinsically two dimensional nature, e.g.: in 1971 [111], in 1972 [112], in 1973 [42], [55], in 1976 [38], in 1977 [33], in 1978 [65], [106], in 1979 [43], [78], in 1980 [17], [66], [79], [108], in 1981 [44], [75], [120], in 1982 [69], [76], [77], [117] and in 1983 [45], [60]. Two dimensional transient simulations of MOSFET's have been carried out in, e.g.:[56], [64] and [122]. Three dimensional static modeling has been published in, e.g.:[12], [39], [89].

In the following chapters particular emphasis will be laid on two phenomena of major importance for MOS-Transistor modeling: these are the influence of surface scattering on carrier mobility and the contribution of impact ionization to carrier generation. The established concepts for device modeling in general are assumed to be familiar to the reader. As basic literature for the newcomer one can suggest the monographs [47], [57] and [83] or the various conference proceedings, e.g.:[3], [8], [9], [10], [24], [54] and [109] or the review papers [6], [28], [31] and [61].

PHYSICAL PREREQUISITES

To be able to write down a set of equations, the "basic" semiconductor equations, one has to go through many non-trivial considerations of solid-state physics and lengthy derivations. The established so-called basic semiconductor equations consist of Poisson's equation (1), the continuity equations for electrons (2) and holes (3) and the current relations for electrons (4) and holes (5).

$$\text{div grad } \psi = \frac{q}{\varepsilon} \cdot (n - p - C) \tag{1}$$

$$\text{div } \vec{J}_n - q \cdot \frac{\partial n}{\partial t} = q \cdot R \tag{2}$$

$$\text{div } \vec{J}_p + q \cdot \frac{\partial p}{\partial t} = -q \cdot R \tag{3}$$

$$\vec{J}_n = q \cdot n \cdot \mu_n \cdot \vec{E}_n + q \cdot D_n \cdot \text{grad } n \tag{4}$$

$$\vec{J}_p = q \cdot p \cdot \mu_p \cdot \vec{E}_p - q \cdot D_p \cdot \text{grad } p \tag{5}$$

To almost this level of completeness, these equations were first presented by VanRoosbroeck [105]. Detailed considerations on the derivation of these basic semiconductor equations can be found in, e.g.,[16], [83], [84].

Models for C, the net doping concentration, for R, the net generation/recombination, and for μ_n, μ_p, the carrier mobilities, are dealt with in detail in the literature (cf. survey of literature in the introduction). $\vec{E}_n$ and $\vec{E}_p$, the effective fields in the current relations are to first order the electric field, however, one may use supplementary correction terms to account for heavy doping or thermally induced currents (cf. [79]). To treat these

second order effects for MOSFET's in more detail goes beyond the scope of this text.

It is obvious that for the sake of simplicity and applicability of any model equations trade-offs between accuracy and complexity have to be taken. Equations (1) to (5) are valid for the major number of engineering applications for silicon devices. But of course there are conditions for which their validity is in doubt or does not exist at all, cf. quantum effects, non-local effects. However, the more sophisticated results in semiconductor physics are too complex to give a rigorous, generally applicable and still sufficiently simple model for the purpose of device simulation.

Surface Scattering

Out of the many scattering effects which the carrier mobility is determined by only surface scattering will be treated here as it is the essential effect in MOSFET's. In theory surface scattering consists of a lot of different mechanisms such as surface roughness scattering, scattering by interface charges, scattering by surface phonons and various quantum effects. Unfortunately, the problems associated with conduction at surfaces have not been investigated as deeply as one would expect. Many physics oriented investigations are carried out at low temperatures because the results can be interpreted much more easily. Therefore, all models which are presently used have been constructed on a fully empirical basis with a scope to reflect the main experimental findings as well as possible.

It was Yamaguchi who suggested one of the earliest models [119]. He has used the formula of Scharfetter and Gummel [72] for lattice scattering, impurity scattering and mobility reduction due to velocity saturation ($\mu_{n,p}^{LIE}$) and an additional factor to reduce the mobility in the presence of an electric field component perpendicular to the current flow direction.

$$\mu_{n,p}^{LIES} = \mu_{n,p}^{LIE} \cdot \frac{1}{\sqrt{1 + \dfrac{|\vec{E} x \vec{J}_{n,p}|}{E_{n,p}^{crit} \cdot |\vec{J}_{n,p}|}}} \qquad (6)$$

$$E_n^{crit} = 6{,}49 \cdot 10^4 \frac{V}{cm}$$
$$E_p^{crit} = 1{,}87 \cdot 10^4 \frac{V}{cm} \tag{7}$$

This model has been used and recommended by many others, too, e.g. [21], [28], [29], [64], because it has been claimed that excellent agreement with experimental results is obtained. However, Thornber [102] has strongly criticized Yamaguchi's treatment using theoretical arguments. The saturation velocity $v_{n,p}^{sat}$ associated with $\mu_{n,p}^{LIE}$ is scaled with the same factor, obviously, as the mobility. Sabnis and Clemens [71] have experimentally proved that surface scattering is almost independent of the doping concentration. Cooper and Nelson [18], [19] have shown with elaborate measurements that the influence of surface fields on the saturation velocity is relatively small, which is in contradiction to former opinions (cf. [40]) but which is quite believable considering their experiments. Very careful measurements on that subject have been published in [92], too. Thornber's suggestion [102] to use a relation of the form (8) for the total effective mobility μ^{LIES} is well accepted today.

$$\mu^{LIES} = \mu^{LIES}(\,\mu^{LIS}(\mu^{LI}, E_\perp),\, E_{||},\, v^{sat}(E_\perp)\,) \tag{8}$$

The function μ^{LIS} combines the mobility due to lattice and ionized impurity scattering with the influence of surface scattering ($E_\perp$ denotes the field component responsible for surface scattering) to a cold carrier mobility, which is then combined with the driving force denoted by $E_{||}$ (usually the field component parallel to the current flow direction or the gradient of the carrier quasi-Fermilevel) and the saturation velocity which might be a function of $E_\perp$ to the total effective mobility μ^{LIES}. μ^{LIS} may have the functional form of (6) as long as good agreement between simulated and measured results is obtained. Yamaguchi, as a matter of fact, has revised his model in a later paper [121] by exactly following the suggestions of Thornber.

I have suggested the following expression for the influence of surface scattering [80], [82].

$$\mu_{n,p}^{LIS} = \mu_{n,p}^{LI} \cdot \frac{x + x_{n,p}^{ref}}{x + b_{n,p} \cdot x_{n,p}^{ref}} \tag{9}$$

x denotes the distance perpendicular to the interface. Directly at the interface (x=0) the mobility is reduced by a factor 1/b; at a distance $x=x^{ref}$ it is reduced by the factor 2/(1+b); and at greater distance from the surface it naturally follows that the reduction factor approaches unity. x^{ref} represents a characteristic length which describes the range of influence of the surface.

$$x_{n,p}^{ref} = \frac{x_{n,p}^{o}}{1 + \frac{E_{n,p}}{E_{n,p}^{crit}}} \tag{10}$$

$$\begin{aligned} x_n^o &= 5\cdot10^{-7}\text{cm} , & E_n^{crit} &= 10^4\frac{V}{cm} \\ x_p^o &= 4\cdot10^{-7}\text{cm} , & E_p^{crit} &= 8\cdot10^3\frac{V}{cm} \end{aligned} \tag{11}$$

This range is modeled as a function of the carrier driving force (field component parallel to current flow or magnitude of the gradient of the corresponding quasi-Fermi potential). The formulation of x^{ref} produces a reduction in the range of influence of surface scattering for greater driving forces, thereby velocity saturation appears. Carriers already traveling with the saturation velocity can be considered not to experience the influence of the surface as much as cold carriers [59]. The parameter "b" in (9) describes the strength of the influence of surface scattering.

$$b_{n,p} = 2 + \frac{E_{\perp}}{E_{\perp n,p}^{crit}} \tag{12}$$

$$E_{\perp n}^{crit} = 1{,}8\cdot10^5\frac{V}{cm} , \qquad E_{\perp p}^{crit} = 3{,}8\cdot10^5\frac{V}{cm} \tag{13}$$

It is modeled as a function of $E_{\perp}$ which can be the electric field component perpendicular to current flow, or the electric field component perpendicular to the interface, or, what I suggest, the projection of the electric field component perpendicular to the current flow direction onto the direction perpendicular to the surface. The formulation of b is based on the fact that the charge carriers are pressed against the surface by an electric field, which results in a greater scattering, in such a way that a greater mobility reduction occurs. Without any electric field one also observes a mobility reduction due to surface roughness scattering (b=2). However, I am absolutely aware that (9) is a fully

phenomenological expression neither of which the structure nor the associated parameters may be claimed to be correct in a theoretical sense. It simply represents my experience which has been confirmed over several years by many users of our simulation tools that an expression with such a structure nicely reflects the experimental observations.

There are plenty more suggestions on how to treat surface scattering phenomenologically. The interested reader could have a look at, e.g., [2], [4], [15], [30], [92], [115].

Impact Ionization

The physical mechanism of major importance for particularly miniaturized MOSFET's in the context of generation/recombination modeling is impact ionization. Two partial processes have to be considered.

a) electron emission: an electron from the valence band moves to the conduction band by consuming the energy of a high energetic electron in the conduction band and leaving a hole in the valence band.
b) hole emission: an electron from the valence band moves to the conduction band consuming the energy of a high energetic hole in the valence band. A hole is left at the valence band edge.

These partial rates can be written:

$$G_n^{II} = \alpha_n \cdot \frac{|\vec{J}_n|}{q} \tag{14}$$

$$G_p^{II} = \alpha_p \cdot \frac{|\vec{J}_p|}{q} \tag{15}$$

The total rate is simply the sum of the partial rates.

$$R^{II} = -G_n^{II} - G_p^{II} \tag{16}$$

α_n and α_p are the ionization rates for electrons and holes defined as generated electron-hole pairs per unit length of travel and per electron and hole, respectively. For instance, an electron generates over a distance $1/\alpha_n$ one electron-hole pair on average. The energy which is consumed from the ionizing carrier is termed ionization energy or threshold energy for ionization E_i. This

quantity has been a subject to a lot of discussions lately with results differing widely. Similarly, the theoretical results for the ionization rates α_n, α_p are not unique. However, both theoretical and experimental investigations indicate a good approximation to be an exponential dependence of the ionization rates upon the electric field component E in direction of current flow.

$$\alpha_n = \alpha_n^{\infty} \cdot \exp\left(-\left(\frac{E_n^{crit}}{E}\right)^{\gamma_n}\right) \tag{17}$$

$$\alpha_p = \alpha_p^{\infty} \cdot \exp\left(-\left(\frac{E_p^{crit}}{E}\right)^{\gamma_p}\right) \tag{18}$$

The exponents γ_n, γ_p are found in the range [1,2]. As a matter of fact fairly early theoretical considerations by Shockley [90] predict the exponents to be one, which has been also the very old experimental finding by Chynoweth [14]. A different treatment by Wolff [118] predicts the exponents to be two. A menu of numerical values for the coefficients of (17) and (18) compiled from literature data is summarized in Table 1 for electrons and in Table 2 for holes. Temperature dependent ionization coefficients which are claimed to perfectly fit measurements have been given in [25], [68].

α_n^{∞} [cm^{-1}]	E_n^{crit} [Vcm^{-1}]	γ_n [ ]	reference	
$1,0 \cdot 10^6$	$1,66 \cdot 10^6$	1	[26]	$1,1 \cdot 10^5 V/cm < E < 5 \cdot 10^5 V/cm$
$6,2 \cdot 10^5$	$1,08 \cdot 10^6$	1	[36]	$2,4 \cdot 10^5 V/cm < E < 5,3 \cdot 10^5 V/cm$
$1,28 \cdot 10^6$	$2,54 \cdot 10^6$	1	[44]	$E < 5 \cdot 10^5 V/cm$
$1 \cdot 10^6$	$5,87 \cdot 10^6$	1	[44]	$E > 5 \cdot 10^5 V/cm$
$1,6 \cdot 10^6$	$1.65 \cdot 10^6$	1	[58]	$2 \cdot 10^5 V/cm < E < 6,7 \cdot 10^5 V/cm$
$3,8 \cdot 10^6$	$1,75 \cdot 10^6$	1	[95], [96]	
$2,2 \cdot 10^6$	$1,54 \cdot 10^6$	1	[99]	
$7 \cdot 10^5$	$1,4 \cdot 10^6$	1	[107]	
$7,03 \cdot 10^5$	$1,231 \cdot 10^6$	1	[110]	$1,75 \cdot 10^5 V/cm < E < 6 \cdot 10^5 V/cm$

Table 1: Constants for impact ionization of electrons

α_p^{∞} $[cm^{-1}]$	E_p^{crit} $[Vcm^{-1}]$	γ_p [ ]	reference	
$2{,}0 \cdot 10^6$	$1{,}98 \cdot 10^6$	1	[36]	$2{,}4 \cdot 10^5 V/cm < E < 5{,}3 \cdot 10^5 V/cm$
$5{,}5 \cdot 10^5$	$1.65 \cdot 10^6$	1	[58]	$5 \cdot 10^5 V/cm < E < 8 \cdot 10^5 V/cm$
$1{,}0 \cdot 10^6$	$1{,}66 \cdot 10^6$	1	[62]	$1{,}1 \cdot 10^5 V/cm < E < 5 \cdot 10^5 V/cm$
$2{,}25 \cdot 10^7$	$3{,}26 \cdot 10^6$	1	[95], [96]	
$1{,}0 \cdot 10^6$	$2{,}22 \cdot 10^6$	1	[99]	
$1{,}3 \cdot 10^6$	$2{,}09 \cdot 10^6$	1	[107]	$E < 6{,}07 \cdot 10^5 V/cm$
$4{,}4 \cdot 10^5$	$1{,}4 \cdot 10^6$	1	[107]	$E > 6{,}07 \cdot 10^5 V/cm$
$1{,}582 \cdot 10^6$	$2{,}036 \cdot 10^6$	1	[110]	$1{,}75 \cdot 10^5 V/cm < E < 4 \cdot 10^5 V/cm$
$6{,}71 \cdot 10^5$	$1{,}693 \cdot 10^6$	1	[110]	$4 \cdot 10^5 V/cm < E < 6 \cdot 10^5 V/cm$

Table 2: Constants for impact ionization of holes

Baraff [7] has claimed these theories to be two limiting cases of a more rigorous model. For low fields Shockley's model is more suitable, whereas for high fields Wolff's model is asymptotically correct. Unluckily, Baraff's results cannot be given in closed form; they have been obtained by a numerical solution of the Boltzmann transport equation, however, restricted to the assumption of an unrealistic band structure. However, a universal plot for both electrons and holes has been presented, which shows

$$\alpha \cdot \lambda = f\left(\frac{E_r}{E_i} , \frac{E_i}{q \cdot \lambda \cdot E} \right) \tag{19}$$

λ is the mean free path between collisions with high energetic phonons; E_r is the average loss of energy defined per such collision; and E_i denotes the ionization energy, as already defined. Numerical values collected from miscellaneous publications are summarized in [79].

Baraff's universal curves have been approximated with compact formulae so that an application for the purpose of simulation becomes easier. The following expression has been suggested by Crowell and Sze [20]:

$$\alpha \cdot \lambda = \exp(C_o(r) + C_1(r) \cdot x + C_2(r) \cdot x^2) \tag{20}$$

with:

$$C_0(r) = -1{,}92 + 75{,}5 \cdot r - 757 \cdot r^2$$

$$C_1(r) = 1{,}75 \cdot 10^{-2} - 11{,}9 \cdot r + 46 \cdot r^2 \qquad (21)$$

$$C_2(r) = 3{,}9 \cdot 10^{-4} - 1.17 \cdot r + 11.5 \cdot r^2$$

where:

$$r = \frac{E_r}{E_i} \qquad x = \frac{E_i}{q \cdot \lambda \cdot E} \qquad (22)$$

This approximation is claimed to be accurate within two percent maximum error over the range $r \in [0.01, 0.06]$ and $x \in [5, 16]$. An even more accurate approximation has been given in [94].

There is still the pending question whether these theoretically obtained results agree with experimental results. The answer to this question is not a trivial one. Provided that one takes the numerical values for λ, E_r and E_i from [20], the measured results of Lee et al. agree satisfactorily with Baraff's results. The experimental results of, e.g. Van Overstraeten et al. [110] and Grant [36], would require totally unrealistic values for λ, E_r and E_i to agree with Baraff's results. On the other hand, in, e.g. [76], [91], [101] the ionization rates of Van Overstraeten et al. have been used, whereby good agreement between experimental and simulation results on device breakdown phenomena has been obtained. The influence of the models for the ionization coefficients upon simulated device performance can be indeed very pronounced [1].

Chwang et al.[13] have rigorously obtained the same results as Baraff with a completely different approach for the calculation, however, with essentially the same assumptions.

An empirical expression suggested by Thornber [103] has been proved to be consistent with an elaborate momentum and energy scaling theory.

$$\alpha = \frac{E}{E_i} \cdot \exp\left(-\frac{F_j}{\frac{k \cdot T \cdot F_j}{E_i} + E + \frac{E^2}{F_r}}\right) \qquad (23)$$

F_j and F_r are interpreted as threshold fields describing the field at which the ionization energy is reached in one mean free path and

the field at which the phonon energy is reached in one mean free path (cf. [103]). (23) includes the asymptotic behavior of the ionization rate, which has been predicted by Baraff. Thornber states that (23) is the first simple, physical, analytical expression for the ionization coefficient valid for all fields. However, by fitting this expression to the experimental data of, e.g. [36], [110], Thornber himself has obtained unexpected large values for the ionization energies.

Recently it has been tried to calculate the impact ionization coefficients by Monte Carlo methods taking into account a realistic band structure [87], [88], [100]. This interesting work, however, is subject to considerable controversy [11], [37].

In the context of impact ionization in very small devices and for low bias applications one problem, the dark space phenomenon, has to be faced. In regions of a device with a large gradient of the electric field component parallel to current flow all models of impact ionization which we have discussed can be expected to overestimate the ionization rates. The carriers first have to gain an energy on their path through the device which is larger than the threshold energy for ionization before impact ionization can take place. The ionization rate at a specific place, thus, will depend, qualitatively spoken, not only on the local field, but also upon the field distribution in that vicinity. Therefore, the dark space phenomenon is frequently termed a non-local effect, e.g. [67]. A rigorous treatment of this and related phenomena [86] with models consisting of pure differential equations is impossible; it is also inconsistent with the usually assumed current relations because for their derivation moderate gradients for the electric field have been assumed (cf. [84]). In a very recent paper [46] an approach to tackle this problem has been proposed, which is basically an extension of Shockley's "Lucky Electron" model. However, in order to understand the many detailed effects of impact ionization many more experimental and theoretical investigations have to be undertaken.

MATHEMATICAL ANALYSIS

From the many mathematical and numerical problems associated with the solution of the basic semiconductor equations for a specific

device, three particular topics will be treated in the following sections. First of all the boundary conditions involved in MOS-modeling will be outlined, since, from a mathematical point of view, a problem with differential operators is only properly defined with boundary conditions. Secondly, the scaling of the semiconductor equations will be discussed. This problem, though of minor interest to the user of a simulation tool on first glance, gives major decisions for subsequent computations and it is frequently underestimated. Finally, the singular perturbation approach towards a structural analysis of solutions to the basic semiconductor equations is presented. The results of this section give much very usefull information on the appropriate selection of numerical methods for actual computations.

Boundary Conditions

All semiconductor devices are principally three dimensional structures. However, in many cases the device under consideration is intrinsically two or even one dimensional and then one can assume that the partial derivatives of the parameters and of the dependent variables of the basic equations perpendicular to a plane (line) vanish, so reducing the problem by one (two) space dimensions, and, thus, simplifying the numerical solution drastically. The basic semiconductor equations (1) to (5) are then posed in a bounded domain $D \in R^n$ (n=1,2,3) representing the device geometry for the purpose of simulation.

The boundary ∂D of D is piecewise smooth for the two or three dimensional problem; it is represented, trivially, by two points for the one dimensional problem (which is of minor interest for modeling MOSFET's). The boundary can be split in principle into two parts.

$$\partial D = \partial D_P \cup \partial D_A \tag{24}$$

∂D_P represents those parts of the boundary which correspond to real "physical" boundaries like contacts and interfaces to insulating material. ∂D_A consists of artificial boundaries which have to be introduced, for instance, to separate neighboring devices in integrated circuits. This second category of boundaries does, therefore, not correspond to boundaries in the physical sense.

In order to illustrate this classification refer to Fig. 1 which

shows the idealized two-dimensional simulation geometry for a planar MOS transistor.

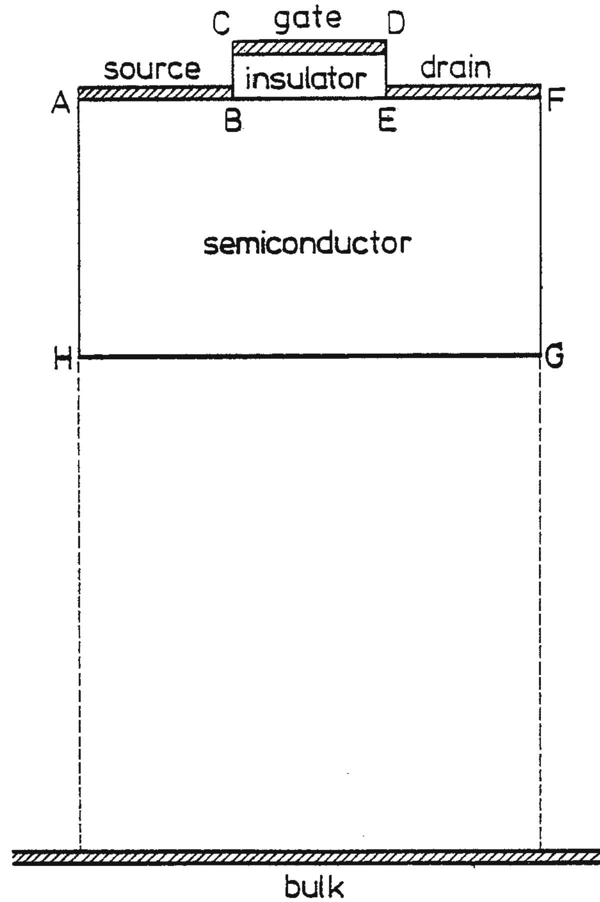

Fig. 1: Idealized simulation geometry of a planar MOSFET

The total domain for the simulation is bounded by the polygon A-B-C-D-E-F-G-H-A. It is obvious that the basic equations (1) to (5) are only posed in the subdomain A-B-E-F-G-H-A. For the insulator (subdomain bounded by B-C-D-E-B), one usually specifies the Laplace equation for the electrostatic potential, and one neglects the existence of any mobile carriers.

$$\text{div grad } \psi = 0 \tag{25}$$

$$n = p = C = 0 \tag{26}$$

One should be aware that by assuming (25) and (26) no gate currents can be calculated and the influence of oxide charges is also neglected. Some considerations on these topics can be found in, e.g., [73], [98], [116].

The boundaries A-B, E-F, C-D and B-E can be interpreted as physical boundaries denoting three idealized contacts and an interface between the semiconductor and the insulator, respectively. These boundaries form ∂D_P. As artificial boundaries A-H, B-C, D-E, F-G and G-H can be identified. These boundaries do not exist in the real device and are only introduced to enable the simulation. It is obvious that these boundaries are not introduced completely arbitrarily. Having a priori information about the functioning of a device it is usually possible to define somewhat natural boundaries which separate the device in a self contained manner from its environment. It should be noted that artificial boundaries are sometimes also introduced to simplify the numerical solution of the basic equations. The boundary G-H represents such a boundary piece. Considering the real dimensions of a MOS transistor we know that the length of the interface B-E is on the order of $1\mu m$ whereas the thickness of the wafer, i.e. the distance between the interface and bulk, is about $500\mu m$. Thus, the real geometry is a long, small stripe which has a disastrous impact on many classical numerical solution methods for the basic equations. From knowledge about the operation of the MOS transistor we can deduce that by cutting off the simulation geometry at some sufficiently large distance from the interface (G-H) we introduce only a small error for most operating conditions of the MOS transistor. In particular, the voltage drop between G-H and the bulk contact and the potential distribution along G-H has to be known such that the artificial boundary G-H is an acceptable simplification [76].

∂D_P, the physically motivated part of the boundary, can be roughly split into two classes.

$$\partial D_P = \partial D_O \cup \partial D_I \tag{27}$$

∂D_O denotes the parts of the boundary corresponding to ohmic contacts and ∂D_I are the interfaces to insulating material.

As boundary condition for the electrostatic potential at ohmic contacts we have in general a functional relation between the electrostatic potential and the total current density, which can include first order derivatives with respect to time and the unit vector perpendicular to the boundary and integrals with respect to time and the area of the ohmic contact. We denote this formally with the following implicit relation:

$$g(\psi, \frac{\partial \psi}{\partial t}, I, \frac{\partial I}{\partial t}) = 0 \tag{28}$$

with:

$$I = \int_{\partial D_O} (\vec{J}_n + \vec{J}_p) \cdot d\vec{A} \tag{29}$$

The simplest boundary conditions are obtained for purely voltage or purely current controlled contacts. In this case (28) simplifies to an explicit boundary condition (Dirichlet condition) for the electrostatic potential.

$$\psi(t) - \psi_b - \psi_D(t) \,|_{\partial D_O} = 0 \tag{30}$$

$\psi_D(t)$ denotes the externally applied bias and ψ_b represents the built-in potential.

For a contact ∂D_O which is current controlled in an ideal manner (28) can be given as:

$$\int_{\partial D_O} (\vec{J}_n + \vec{J}_p) \cdot d\vec{A} - I_D(t) = 0 \tag{31}$$

$I_D(t)$ is the total current which is forced to flow through the contact. Substituting the current relations (4) and (5) into the boundary condition (31) one obtains an integral boundary condition. However, an additional condition is required to avoid ambiguities since only the electric field and not the electrostatic potential enters in the boundary condition. One usually assumes that the ohmic contact is ideally conducting which means that there is no voltage drop in the boundary.

$$\psi(t) - \psi_b \,|_{\partial D_O} = \text{const.} \tag{32}$$

The derivatives with respect to time of the electric field and the total current enter into the boundary condition for the case of a capacitive, or inductive load. The boundary conditions for a given external load circuit are, with some knowledge about circuit theory, similarly to derive as for ideal current drive. In the mathematical sense one will obtain a fairly complex time dependent boundary condition.

As boundary conditions for the carrier densities it is well established, although a matter open to physical criticism, to assume thermal equilibrium (which corresponds to infinite surface recombination velocities) and vanishing space charge at ohmic contacts.

$$n \cdot p - n_i^2 = 0 \tag{33}$$

$$n - p - C = 0 \tag{34}$$

These two conditions can be rearranged into Dirichlet boundary conditions for electrons and holes.

The second category of boundaries in (27) are the interfaces ∂D_I between the semiconductor and insulating material. At such interfaces the law of Gauss in differential form must be obeyed.

$$\varepsilon_{sem} \cdot \frac{\partial \psi}{\partial \vec{n}}\Big|_{sem} - \varepsilon_{ins} \cdot \frac{\partial \psi}{\partial \vec{n}}\Big|_{ins} = Q_{int} \tag{35}$$

$\vec{n}$ denotes the unit normal vector on ∂D which exists almost everywhere (that is, everywhere except on a subset of ∂D of Lebesque measure zero). Practically, $\vec{n}$ possibly does not exist on a finite number of edges.

ε_{sem} and ε_{ins} are the permittivity in the semiconductor and the insulator, respectively. Q_{int} represents charges at the interface. For interfaces to a thick insulator, e.g. field oxide, one frequently assumes in the insulator a vanishing electric field component perpendicular to the interface, so that (35) simplifies to:

$$\varepsilon_{sem} \cdot \frac{\partial \psi}{\partial \vec{n}}\Big|_{sem} = Q_{int} \tag{36}$$

Quite often the existence of interface charges is also neglected. (36) then reduces to a Neumann boundary condition for the electrostatic potential. In several MOS simulation programs the Laplace equation is not solved explicitly in the insulator. Instead a one dimensional potential drop perpendicular to the interface is assumed which leads to a mixed boundary condition for the electrostatic potential at the interface:

$$\varepsilon_{sem} \cdot \frac{\partial \psi}{\partial \vec{n}}\Big|_{sem} - \varepsilon_{ins} \cdot \frac{U_G - \psi}{t_{ins}} = Q_{int} \tag{37}$$

U_g denotes the electrostatic potential at the gate contact C-D; t_{ins} is the thickness of the insulator C-B. It is obvious that it is much easier to program the mixed boundary condition (37) instead of solving the Laplace equation in the insulator. However, if the length of the interface B-E is not extraordinarily large compared to the thickness of the insulator the error introduced is, from my own personal experience, intolerably large.

For the continuity equations the current components perpendicular to the interface must equal the surface recombination rate R^{SURF}.

$$\vec{J}_n \cdot \vec{n} = -q \cdot R^{SURF} \tag{38}$$

$$\vec{J}_p \cdot \vec{n} = q \cdot R^{SURF} \tag{39}$$

Quite frequently the existence of surface recombination is simply ignored by assuming vanishing surface recombination velocities. Under certain circumstances, depending on the specific device and its operating conditions, this can be justified.

For the artificial boundaries in (24) one assumes either the natural boundary conditions (Neumann conditions) which guarantee that the domain under consideration, i.e. the simulated device area, is self contained (40), or one specifies Dirichlet values for the electrostatic potential and the carrier densities, which are a priori estimated (e.g. at G-H in Fig. 1).

$$\frac{\partial \psi}{\partial \vec{n}} = 0 \ , \quad \frac{\partial n}{\partial \vec{n}} = 0 \ , \quad \frac{\partial p}{\partial \vec{n}} = 0 \tag{40}$$

The applicability of these boundary conditions has to be justified by physical and mathematical reasoning. In Fig. 1, for instance, the distances A-B and E-F must be sufficiently large that the error introduced by the artificial boundary conditions at A-H and F-G is tolerably small. A definite requirement for the applicability of the boundary conditions (40) is that the derivatives of the parameters C, D_n, D_p, μ_n and μ_p with respect to the unit normal vector at the boundary vanish along the artificial boundary.

It is to note that the basic semiconductor equations only constitute a time dependent problem if the boundary condition for the electrostatic potential is time dependent. If the boundary condition for the electrostatic potential is time invariant the semiconductor equations reduce to a system of three coupled elliptic equations.

Scaling

Since the dependent variables (ψ,n,p) in the basic equations (1) to (5) are of greatly different orders of magnitude and show a strongly different behavior in regions with small and large space charge, the first step towards a structural analysis of the basic equations has

to be appropriate scaling. A standard way of scaling which was established for many years has been given by DeMari [22], [23], However, a scaling which is more rigorous from the mathematical point of view has been introduced in [113], [114] and further developed in [49], [50]. The factors for this scaling are summarized in Table 3.

quantity	symbol	value
$\vec{x}$	x_o	$\max\lvert\vec{x}-\vec{y}\rvert,\ \vec{x},\vec{y} \in D$
ψ	ψ_o	$k \cdot T/q$
n,p,C	C_o	$\max\lvert C(\vec{x})\rvert,\ \vec{x} \in D$
D_n,D_p	D_o	$\max(D_n(\vec{x}),D_p(\vec{x})),\ \vec{x} \in D$
μ_n,μ_p		D_o/ψ_o
R		$D_o \cdot C_o/x_o^2$
t		x_o^2/D_o

Table 3: Scaling Factors

The basic equations will transform with this scaling (after substituting (4) into (2) and (5) into (3), respectively) into:

$$\lambda^2 \cdot \operatorname{div} \operatorname{grad} \psi - (n - p - C) = 0 \tag{41}$$

$$\operatorname{div} (D_n \cdot \operatorname{grad} n - \mu_n \cdot n \cdot \operatorname{grad} \psi) - R(\psi,n,p) = \frac{\partial n}{\partial t} \tag{42}$$

$$\operatorname{div} (D_p \cdot \operatorname{grad} p + \mu_p \cdot p \cdot \operatorname{grad} \psi) - R(\psi,n,p) = \frac{\partial p}{\partial t} \tag{43}$$

with:

$$\lambda^2 = \frac{\psi_o \cdot \varepsilon}{x_o^2 \cdot q \cdot C_o} \tag{44}$$

All quantities in (41) to (43) are scaled. The differential operators are taken with respect to the scaled independent variables. For the sake of transparency, however, an explicit indication (e.g. an index) has been omitted. Furthermore, the equations (41) to (43) have been multiplied with combinations of the scaling factors, namely:

$\dfrac{\varepsilon}{q \cdot C_o}$ for (1)

$\dfrac{x_o^2}{D_o \cdot C_o}$ for (2), (3)

Note, that in the scaled Poisson equation (41) the space charge is scaled to maximally O(1) which allows to take directly the residuals of (41) as a measure of the computational accuracy for actual computations. Analogous statements hold for the continuity equations.

The parameter λ^2 in (41) is a very small constant; its numerical value is in the order of 10^{-10} to 10^{-6}. By physically reasoning λ can be identified as the scaled minimum Debye length in the device. The fact that the Laplacian in the Poisson equation is multiplied with a very small constant enables an asymptotic analysis of the basic semiconductor equations by means of singular perturbation theory. This will be the topic of the next section.

It should be noted that for high voltage problems it is preferable to scale the electrostatic potential with the maximum applied bias instead of the thermal voltage $k \cdot T/q$. Such a modification of the scaling has only a minor impact on the following analysis of the basic equations. However, in view of computational aspects it is advantageous since all scaled dependent variables are then maximally O(1).

The Singular Perturbation Approach

The scaled basic semiconductor equations (41) to (43) constitute a singularly perturbed boundary value problem with perturbation parameter λ [51]. This interpretation is attractive because it allows the application of classical strategies for the qualitative analysis of the basic equations, e.g. [27], [32].

At first one usually tries to solve a singularly perturbed problem by a regular expansion in λ, the perturbation parameter. For the semiconductor equations this yields:

$$w(\vec{x},t,\lambda) = \sum_{i=0}^{\infty} \tilde{w}_i(\vec{x},t) \cdot \lambda^i \tag{45}$$

with:

$$w = \begin{pmatrix} \psi \\ n \\ p \end{pmatrix} \tag{46}$$

The $\tilde{w}_i(\vec{x},t)$ are independent of λ and shall represent "slowly varying" quantities (slow compared to the variation of the doping

profile across pn-junctions). Such an expansion implies a smooth dependence of the solution upon λ. By inserting (45) into equations (41) to (43) and setting λ equal to zero we obtain the so-called reduced problem.

$$\tilde{n}_o - \tilde{p}_o - C = 0 \tag{47}$$

$$\text{div}\,(D_n \cdot \text{grad}\,\tilde{n}_o - \mu_n \cdot \tilde{n}_o \cdot \text{grad}\,\tilde{\psi}_o) - R(\tilde{\psi}_o, \tilde{n}_o, \tilde{p}_o) = \frac{\partial \tilde{n}_o}{\partial t} \tag{48}$$

$$\text{div}\,(D_p \cdot \text{grad}\,\tilde{p}_o + \mu_p \cdot \tilde{p}_o \cdot \text{grad}\,\tilde{\psi}_o) - R(\tilde{\psi}_o, \tilde{n}_o, \tilde{p}_o) = \frac{\partial \tilde{p}_o}{\partial t} \tag{49}$$

In semiconductor device physics this problem is called the charge-neutral approximation and has proved to be very valuable. Note, that it has been derived here very formally. However, as we have mentioned before the net doping distribution C varies rapidly; actually, it changes almost abruptly at pn-junctions. Therefore, the expansion (45) is insufficient to describe solutions of the basic equations completely. We can see this from relation (47) which cannot be fulfilled with slowly varying quantities $\tilde{n}_o$, $\tilde{p}_o$ for rapidly changing C.

A pn-junction can be described in more mathematical terms as a n-1 dimensional manifold Γ (n denotes the number of space dimensions) which splits the domain into two subdomains. If there exists more than one pn-junction in a device, which usually is the case, the simulation domain has to be split into subdomains whose "inner" boundaries represent the pn-junction. Since the procedure to be outlined in the following is the same for each of the junctions it is demonstrated for one pn-junction only, without loss of generality. By partitioning the simulation geometry along the pn-junction into subdomains the net doping concentration C does not change sign within each of the subdomains. Furthermore, one splits the doping profile within each subdomain into two parts:

$$C = \tilde{C} + \hat{C} \tag{50}$$

$\tilde{C}$ represents the slowly varying (within the subdomain) contribution to the doping concentration, and $\hat{C}$ is rapidly (typically exponentially) decaying to zero away from the pn-junction. For an ideal abrupt junction $\hat{C}$ would be zero. We replace now the total doping concentration C in (47) by the smooth part $\tilde{C}$.

$$\tilde{n}_o - \tilde{p}_o - \tilde{C} = 0 \tag{51}$$

As the expansion (45) is inappropriate to describe the full solution in the vicinity of a pn-junction Γ it has to be supplemented by "layer" terms according to singular perturbation theory.

$$w(\vec{x},t,\lambda) = \sum_{i=0}^{\infty} (\tilde{w}_i(\vec{x},t) + \hat{w}_i(r,\frac{s}{\lambda},t))\cdot\lambda^i \qquad (52)$$

The following coordinates have been employed. $r=r(\vec{x})$ is the point on the pn-junction Γ closest to $\vec{x}$; $s=s(\vec{x})$ denotes the distance between $\vec{x}$ and Γ.

If one evaluates the scaled continuity equations (42) and (43) after substituting (52) and carrying out the differentiation, one obtains, by comparing coefficients of order $O(\lambda^{-1})$, a system of ordinary differential equations in $(\hat{\psi}_o,\hat{n}_1,\hat{p}_1)$ (cf. [53]). The quantities $\hat{n}_o$, $\hat{p}_o$ vanish which means that no zero order internal layers exist.

In order to define the reduced problem completely, four "interface conditions" have to be additionally imposed on the two second order equations (48) and (49) at the pn-junction Γ. These are obtained by matching the full solution (52) at the pn-junction [SO36]. The solution of the reduced problem is an $O(\lambda)$ approximation to the full solution away from Γ. This reduced problem is a valuable tool for the development and analysis of numerical solution methods for the full problem, since the reduced problem has to be solved implicitly by any discretization method which should deliver sufficient accuracy for a reasonable number of grid points [81], [85].

One crucial point in these considerations is the behavior of the solution of the full problem and of the expansion (52) close to the boundary ∂D. By setting λ equal to zero we lose one degree of freedom in imposing boundary conditions. Therefore, the reduced solution will only be close to the full solution near those parts of the boundary ∂D where the boundary conditions do not contradict the algebraic equation (51) [53]. This is the case for ideal ohmic contacts, but not for interfaces where large normal components of the electric field occur, which lead to boundary layers [52], i.e. MOS inversion layer. However, one can overcome this problem by adding to the boundary layers at interfaces layer terms in (52) in a similar manner as has been done for the internal layers at pn-junctions [53], [SO36]. Anyway, the reduced solution will for many applications (numerical computations) serve as an excellent initial guess for the full solution, as has been confirmed by numerical experiments [34].

EXAMPLES OF PROPER MODEL APPLICATION

The next sections are devoted to two typical examples of applications of simulation programs. At first the influence of lightly-doped-drain (LDD) on impact ionization in a miniaturized planar MOSFET will be pinpointed. The simulations for this purpose have been carried out with the MINIMOS program [77], [79]. Secondly, the behavior of holes in a vertical MOSFET, a SIPMOS transistor [104], close to breakdown will be sketched. For this example the simulations have been performed with the BAMBI program [35].

Impact ionization in LDD MOSFET's

New concerns about degradation of transistor characteristics due to impact ionization are introduced by the scaling of feature sizes in VLSI devices. Therefore, many process modifications have been suggested to either reduce the peak electric field in the drain region or to shift the region of the peak electric field from underneath the gate electrode more down into the bulk, e.g., [93], [97]. One such concept is based on having lightly doped drains (LDD). It is intuitively expected that MOSFET's with LDD are less sensitive to impact ionization than conventional devices. However, only little data has been published on the real performance bargain obtained by the LDD concept [5].

To outline the influence of the LDD on the peak electric field and the impact ionization rate two transistors each with 1μm channel length have been simulated. The doping profile of these transistors is shown in Fig. 2. To give a better visibility only one half of the transistors, starting from the middle of the channel up to the heavily doped drain area, has been drawn.

In Fig. 3 the lateral component of the electric field, i.e. the component parallel to the interface is shown. The windows of the drawings are the same as for the doping profiles. The peak electric field is reduced from $6.4 \cdot 10^{-5}$V/cm in the conventional structure to $3.3 \cdot 10^{-5}$V/cm in the device with the LDD at the bias conditions (UGS=1V, UDS=5V). The success of the LDD on reducing the peak electric field is clearly demonstrated thereby.

without LDD with LDD

Fig. 2: Doping profile, log.scale, $[cm^{-3}]$

without LDD with LDD

Fig. 3: lateral component of electric field, lin.scale, [V/cm]

Fig. 4 shows the impact ionization rates for the two transistors. The maximum ionization rate is reduced from $4.2 \cdot 10^{28}$ pairs per cubic centimeter and second to about $1.3 \cdot 10^{27} cm^{-3} s^{-1}$. Furthermore the area covered by impact ionization is also smaller in the LDD device

and the behavior close to the maximum is much smoother. Therefore, a non-neglible reduction of the substrate current (about 75%) can be observed.

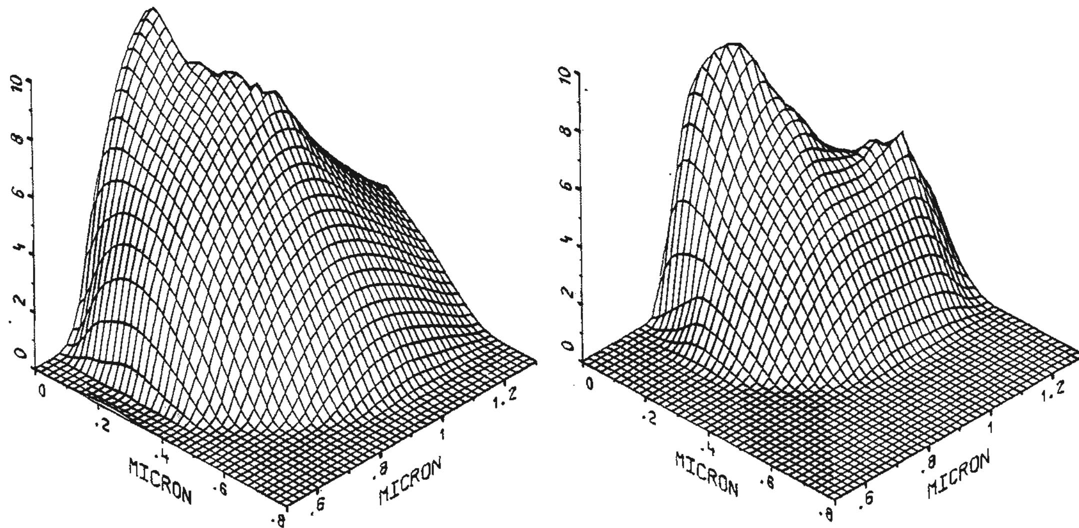

without LDD with LDD

Fig. 4: Impact ionization rate,
scale: $-\mathrm{sign}(R)\cdot\log(1+|R|/10^{18}\mathrm{cm}^{-3}\mathrm{s}^{-1})$, [ ]

The Behavior of Holes in SIPMOS Devices

Since the field of applications of power MOS-Transistors has significantly broadened in recent years, one example of power MOSFET modeling will be sketched in the following. The question of the behavior of the hole concentration in a 100V SIPMOS transistor has been investigated for this purpose. Three operating points at a gate bias of UGS=6V and drain biases of UDS=50V, 100V and 150V, respectively, have been calculated. Fig. 5 shows the doping profile of the device under consideration. The epilayer thickness of the n^- drain has been designed to safely block 100V.

Fig. 6, Fig. 8 and Fig. 10 show the magnitude of the electron current density for the chosen operating conditions. One can nicely see that the current is injected from the inversion channel into a fairly narrow path. In the lowly doped epilayer the current density spreads expectedly. The maximum of the current density is certainly found in the inversion channel at the interface.

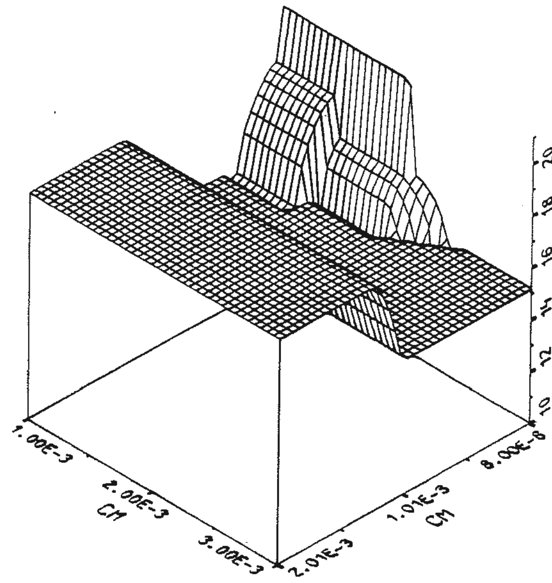

Fig. 5: Doping profile of SIPMOS Transistor, log.scale, [cm^{-3}]

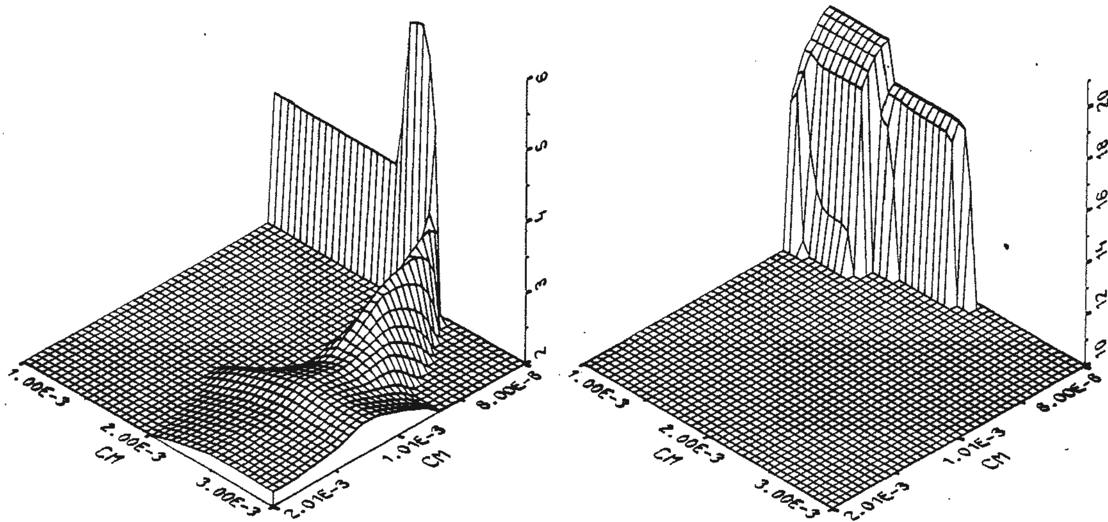

(UGS=6V, UDS=50V)

Fig. 6: Magnitude of electron current density, log.scale, [A/cm^2]

Fig. 7: Concentration of holes, log.scale, [cm^{-3}]

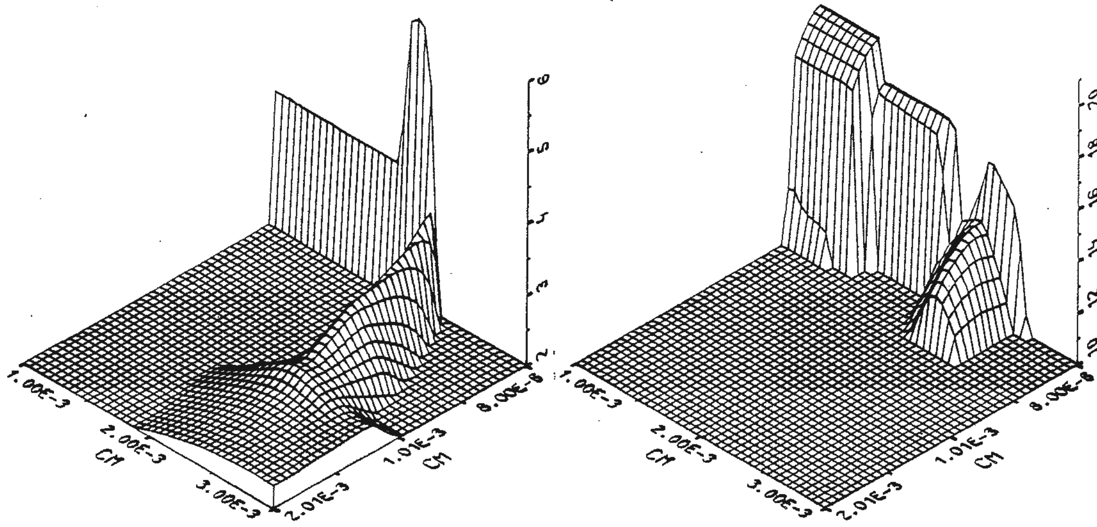

(UGS=6V, UDS=100V)

Fig. 8: Magnitude of electron current density, log.scale, [A/cm^2]

Fig. 9: Concentration of holes, log.scale, [cm^{-3}]

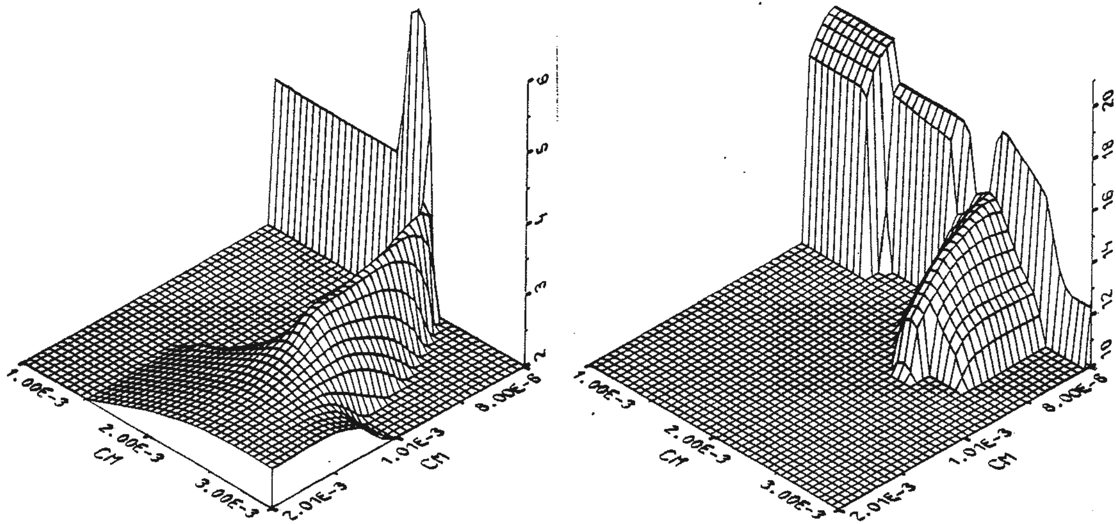

(UGS=6V, UDS=150V)

Fig. 10: Magnitude of electron current density, log.scale, [A/cm^2]

Fig. 11: Concentration of holes, log.scale, [cm^{-3}]

Fig. 7, Fig, 9 and Fig. 11 show the hole concentration at UDS=50V, 100V and 150V, respectively. At UDS=50V no holes are yet generated by impact ionization; this operating point can therefore serve as a reference. At UDS=100V one can see a non-negligible amount of holes being generated in the epilayer close to the channel region. The hole current contributes at this bias condition with about 15% to the total drain current. At UDS=150V the hole concentration generated by impact ionization is larger than the doping concentration of the epilayer. The device is very close to breakdown. The hole current exceeds 30% of the total drain current. From Fig. 12 showing the magnitude of the hole current density we can deduce that the holes flow to some extent to the interface forming an accumulation layer but to a larger extent they flow directly towards the p^+ region where they are collected by the source contact which overlaps the p-doped area.

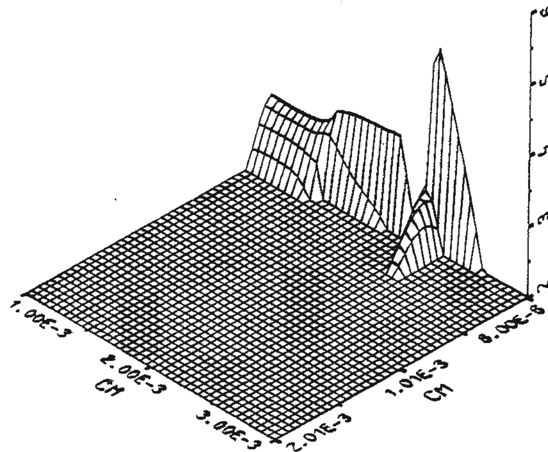

(UGS=6V, UDS=150V)
Fig. 12: Magnitude of hole current density, log.scale, $[A/cm^2]$

A last remark should be made about the negative differential output conductance which SIPMOS devices and similar vertical power MOSFET's exhibit for high gate bias. This phenomenon could not be observed in simulated characteristics obtained by the BAMBI program. Since the heat flow equation is not solved self-consistently with the

semiconductor equations by BAMBI, but a constant temperature is assumed all over the device, one may speculate this negative differential conductance to be caused by a thermal effect. The fairly narrow electron current path (cf. Fig. 6, Fig. 8, Fig. 10) might be heated locally by the high current densities which decreases the current and, thus, leads to a negative differential conductance [70].

CONCLUSION

Some aspects of modern MOSFET modeling have been reviewed. It should be explicitly stated that progress in this field can only be expected if progress in the understanding of the basic physical phenomena of carrier transport in MOSFET's is achieved. The mathematical prerequisites to model MOS-Transistors are sufficiently developed to carry out simulations for research purpose with a considerable, but acceptable amount of computer resources. However, as simulation programs improve in scope, reliability and accuracy, it can be expected that their use to aid device development will still significantly increase.

ACKNOWLEDGEMENT

I am in dept to Prof.H.Pötzl for many stimulating discussions and critically reading my manuscript. Considerable support has been granted by Siemens AG, Munich and by the "Fonds zur Förderung der wissenschaftlichen Forschung" (Project Nr.S43/10). I thank all of my colleages, particularly Dr.A.Franz and Doz.P.Markowich, who have contributed to much of the material presented herein. Excellent computer access has been provided by Dipl.Ing.D.Schornböck with assistence of the whole staff of the computer center.

REFERENCES

[1] Adler M.S., Temple V.A.K., Rustay R.C., "Theoretical Basis for Field Calculations on Multi-Dimensional Reverse Biased Semiconductor Devices", Solid-State Electron., 25 (1982) 1179-1186.

[2] Akers L.A., Portnoy W.M., "Numerical Analysis of the Steady-State Behaviour of a MOS Field Effect Transistor", Int.J.Numer.Meth.Eng., 15 (1980) 1221-1238.

[3] Antognetti P., Antoniadis D.A., Dutton R.W., Oldham W.G., "Process and Device Simulation for MOS-VLSI Circuits", (Martinus Nijhoff, The Hague, 1983).

[4] Baccarani G., Wordeman M.R., "Transconductance Degradation in Thin-Oxide MOSFETs", Proc.IEDM (1982) 278-281.

[5] Baglee D.A., Duvvury C., "Reduced Hot-Electron Effects in MOSFET's with an Optimized LDD Structure", IEEE Electron Device Lett., **EDL-5** (1984) 389-391.

[6] Bank R.E., Rose D.J., Fichtner W., "Numerical Methods for Semiconductor Device Simulation", IEEE Trans.Electron Devices, **ED-30** (1983) 1031-1041.

[7] Baraff G.A., "Distribution Functions and Ionization Rates for Hot Electrons in Semiconductors", Physical Review, **128** (1962) 2507-2517.

[8] Board K., Owen D.R.J., "Simulation of Semiconductor Devices and Processes", (Pineridge Press, Swansea, 1984).

[9] Browne B.T., Miller J.J.H., "Numerical Analysis of Semiconductor Devices", (Boole Press, Dublin, 1979).

[10] Browne B.T., Miller J.J.H., "Numerical Analysis of Semiconductor Devices and Integrated Circuits", (Boole Press, Dublin, 1981).

[11] Capasso F., Pearsall T.P., Thornber K.K., "The Effect of Collisional Broadening on Monte Carlo Simulations of High-Field Transport in Semiconductor Devices", IEEE Electron Device Lett., **EDL-2** (1981) 295.

[12] Chamberlain S.G., Husain A., "Three-Dimensional Simulation of VLSI MOSFET's", Proc.IEDM (1981) 592-595.

[13] Chwang R., Kao C.K., Crowell C.R., "Normalized Theory of Impact Ionization and Velocity Saturation in Nonpolar Semiconductors via a Markov Chain Approach", Solid-State Electron., **22** (1979) 599-620.

[14] Chynoweth A.G., "Ionization Rates for Electrons and Holes in Silicon", Physical Review, **109** (1958) 1537-1540.

[15] Coen R.W., Muller R.S., "Velocity of Surface Carriers in Inversion Layers on Silicon", Solid-State Electron., **23** (1980) 35-40.

[16] Coffey W.T., Vij J.K., "On the Origin of the Nonlinear Equations for the Potential and Current Density in a Semiconductor", in: Finite Element Programming with Special Emphasis on Semiconductor Device and Process Modelling (Boole Press, Dublin, 1983) 24-40.

[17] Colak S., Singer B., Stupp E., "Lateral DMOS Power Transistor Design", IEEE Electron Device Lett., **EDL-1** (1980) 51-53.

[18] Cooper J.A., Nelson D.F., "Measurement of the High-Field Drift Velocity of Electrons in Inversion Layers on Silicon", IEEE Electron Device Lett., **EDL-2** (1981) 171-173.

[19] Cooper J.A., Nelson D.F., "High-Field Drift Velocity of Electrons at the Si-SiO2 Interface as Determined by a Time-of-Flight Technique", J.Appl.Phys., **54** (1983) 1445-1456.

[20] Crowell C.R., Sze S.M., "Temperature Dependence of Avalanche Multiplication in Semiconductors", Appl.Phys.Lett., **9** (1966) 242-244.

[21] D'Avanzo D.C., Vanzi M., Dutton R.W., "One-Dimensional Semiconductor Device Analysis (SEDAN)", Report G-201-5 (Stanford University, 1979).

[22] DeMari A., "An Accurate Numerical Steady-State One-Dimensional Solution of the P-N Junction", Solid-State Electron., **11** (1968) 33-58.

[23] DeMari A., "An Accurate Numerical One-Dimensional Solution of the P-N Junction under Arbitrary Transient Conditions", Solid-State Electron., **11** (1968) 1021-2053.

[24] DeMeyer K.M., "VLSI Process and Device Modeling", (Katholieke Universiteit Leuven, 1983).

[25] Decker D.R., Dunn C.N., "Temperature Dependence of Carrier Ionization Rates and Saturated Velocities in Silicon", J.Electronic Mat., **4** (1975) 527-547.

[26] Dziewior J., Schmid W., "Auger Coefficients for Highly Doped and Highly Excited Silicon", Appl.Phys.Lett., **31** (1977) 346-348.

[27] Eckhaus W., "Asymptotic Analysis of Singular Perturbations", (North-Holland, Amsterdam, 1979).

[28] Engl W.L., Dirks H.K., Meinerzhagen B., "Device Modeling", Proc.IEEE, **71** (1983) 10-33.

[29] Engl W.L., Dirks H., "Models of Physical Parameters", in: Introduction to the Numerical Analysis of Semiconductor Devices and Integrated Circuits (Boole Press, Dublin 1981) 42-46.

[30] Ezawa H., "Inversion Layer Mobility with Intersubband Scattering", Surface Science, **58** (1976) 25-32.

[31] Fichtner W., Rose D.J., Bank R.E., "Semiconductor Device Simulation", IEEE Trans.Electron Devices, **ED-30** (1983) 1018-1028.

[32] Fife P.C., "Semilinear Elliptic Boundary Value Problems with Small Parameters", Arch.Rational Mech.Anal., **52** (1973) 205-232.

[33] Fortino A.G., Nadan J.S., "An Efficient Method for the Small-Signal AC Analysis of MOS Capacitors", IEEE Trans.Electron Devices, **ED-24** (1977) 1137-1147.

[34] Franz A.F., Franz G.A., Selberherr S., Ringhofer C., Markowich P., "Finite Boxes - A Generalization of the Finite Difference Method Suitable for Semiconductor Device Simulation", IEEE Trans.Electron Devices, **ED-30** (1983) 1070-1082.

[35] Franz A.F., Franz G.A., Selberherr S., "BAMBI - A Design Model for Power MOSFET's", Proc.Int.Conf.CAD (1984) 179-181.

[36] Grant W.N., "Electron and Hole Ionization Rates in Epitaxial Silicon at High Electric Fields", Solid-State Electron., **16.** (1973) 1189-1203.

[37] Hess K., "Comment on "Effect of Collisional Broadening on Monte Carlo Simulations of High -Field Transport in Semiconductor Devices"", IEEE Electron Device Lett., **EDL-2** (1981) 297-298.

[38] Hori R., Masuda H., Minato O., Nishimatu S., Sato K., Kubo M., "Short Channel MOS-IC Based on Accurate Two Dimensional Device Design", Jap.J.Appl.Phys., **15** (1976) 193-199.

[39] Husain A., Chamberlain S.G., "Three-Dimensional Simulation of VLSI MOSFET's: The Three-Dimensional Simulation Program WATMOS", IEEE J.Solid-State Circuits, **SC-17** (1982) 261-268.

[40] Jacoboni C., Canali C., Ottaviani G., Quaranta A.A., "A Review of Some Charge Transport Properties of Silicon", Solid-State Electron., **20** (1977) 77-89.

[41] Kahng D., Atalla M.M., "Silicon-Silicondioxide Field Induced Surface Devices", Proc.IRE-AIEE Solid-State Dev.Res.Conf. (1960).

[42] Kennedy D.P., Murley P.C., "Steady State Mathematical Theory for the Insulated Gate Field Effect Transistor", IBM J.Res.Dev., **17** (1973) 2-12.

[43] Kotani N., Kawazu S., "Computer Analysis of Punch-Through in MOSFET's", Solid-State Electron., **22** (1979) 63-70.

[44] Kotani N., Kawazu S., "A Numerical Analysis of Avalanche Breakdown in Short-Channel MOSFET's", Solid-State Electron., **24** (1981) 681-687.

[45] Kotani N., Kawazu S., Komori S., "Behavior of Holes Generated by Impact Ionization in n-Channel MOSFET's", IEEE Trans.Electron Devices, **ED-30** (1983) 1678-1680.

[46] Kuhnert R., Werner C., Schütz A., "A Novel Impact-Ionization Model for 1um MOSFET Simulation", IEEE Trans.Electron Devices, **ED-32** (1985).

[47] Kurata M., "Numerical Analysis for Semiconductor Devices", (Lexington, Massachusetts, 1982).

[48] Loeb H.W., Andrew R., Love W., "Application of 2-Dimensional Solutions of the Shockley-Poisson Equation to Inversion-Layer M.O.S.T. Devices", Electron.Lett., **4** (1968) 352-354.

[49] Markowich P.A., Ringhofer C.A., Selberherr S., Langer E., "A Singularly Perturbed Boundary Value Problem Modelling a Semiconductor Device", Report 2388 (MRC, University of Wisconsin, 1982).

[50] Markowich P.A., Ringhofer C.A., Langer E., Selberherr S., "An Asymptotic Analysis of Single-Junction Semiconductor Devices", Report 2527 (MRC, University of Wisconsin, 1983).

[51] Markowich P.A., Ringhofer C.A., Selberherr S., "A Singular Perturbation Approach for the Analysis of the Fundamental Semiconductor Equations", Report 2482 (MRC, University of Wisconsin, 1983).

[52] Markowich P.A., "A Singular Perturbation Analysis of the Fundamental Semiconductor Device Equations", Habilitation (Technische Universität Wien, 1983).

[53] Markowich P.A., "A Qualitative Analysis of the Fundamental Semiconductor Device Equations", COMPEL, **2** (1983) 97-115.

[54] Miller J.J.H., "Numerical Analysis of Semiconductor Devices and Integrated Circuits", (Boole Press, Dublin, 1983).

[55] Mock M.S., "A Two-Dimensional Mathematical Model of the Insulated-Gate Field-Effect Transistor", Solid-State Electron., **16** (1973) 601-609.

[56] Mock M.S., "A Time-Dependent Numerical Model of the Insulated-Gate Field-Effect Transistor", Solid-State Electron., **24** (1981) 959-966.

[57] Mock M.S., "Analysis of Mathematical Models of Semiconductor Devices", (Boole Press, Dublin, 1983).

[58] Moll J.L., VanOverstraeten R., "Charge Multiplication in Silicon p-n Junctions", Solid-State Electron., **6** (1963) 147-157.

[59] Müller W., Risch L., Schütz A., "Analysis of Short Channel MOS Transistors in the Avalanche Multiplication Regime", IEEE Trans.Electron Devices, **ED-29** (1982) 1778-1784.

[60] Navon D.H., Wang C.T., "Numerical Modeling of Power MOSFET's", Solid-State Electron., **26** (1983) 287-290.

[61] Newton A.R., "Computer-Aided Design of VLSI Circuits", Proc.IEEE, **69** (1981) 1189-1199.

[62] Ogawa T., "Avalanche Breakdown and Multiplication in Silicon pin Junctions", Jap.J.Appl.Phys., **4** (1965) 473-484.

[63] Ogura S., Tsang P.J., Walker W.W., Critchlow D.L., Shepard J.F., "Design and Characteristics of the Lightly Doped Drain-Source (LDD) Insulated Gate Field-Effect Transistor", IEEE Trans.Electron Devices, **ED-27** (1980) 1359-1367.

[64] Oh S.Y., Ward D.E., Dutton R.W., "Transient Analysis of MOS Transistors", IEEE Trans.Electron Devices, **ED-27** (1980) 1571-1578.

[65] Oka H., Nishiuchi K., Nakamura T., Ishikawa H., "Two-Dimensional Numerical Analysis of Normally-Off Type Buried Channel MOSFET's", Proc.IEDM (1979) 30-33.

[66] Oka H., Nishiuchi K., Nakamura T., Ishikawa H., "Computer Analysis of a Short-Channel BC MOSFET", IEEE Trans.Electron Devices, **ED-27** (1980) 1514-1520.

[67] Okuto Y., Crowell C.R., "Ionization Coefficients in Semiconductors: A Nonlocalized Property", Physical Review, **B10** (1974) 4284-4296.

[68] Okuto Y., Crowell C.R., "Threshold Energy Effect on Avalanche Breakdown Voltage in Semiconductor Junctions", Solid-State Electron., **18** (1975) 161-168.

[69] Rahali F., "Analyse Numerique a 2 Dimensions de Transistors MOS par la Methode des Elements Finis", (Laboratoire d'electronique generale, Lausanne, 1982).

[70] Rossel P., "Power MOS Devices", Microelectron.Reliab., **24** (1984) 339-366.

[71] Sabnis A.G., Clemens J.T., "Characterization of the Electron Mobility in the Inverted (100) SI-Surface", Proc.IEDM (1979) 18-21.

[72] Scharfetter D.L., Gummel H.K., "Large-Signal Analysis of a Silicon Read Diode Oscillator", IEEE Trans.Electron Devices, **ED-16** (1969) 64-77.

[73] Schmitt-Landsiedel D., "Physikalisch begrenzende Parameter bei der Transistorverkleinerung: Dünne Oxide und heisse Elektronen", Dissertation (Technische Universität München, 1984).

[74] Schroeder J.E., Muller R.S., "IGFET Analysis Through Numerical Solution of Poisson's Equation", IEEE Trans.Electron Devices, **ED-15** (1968) 954-961.

[75] Schütz A., Selberherr S., Pötzl H.W., "Numerical Analysis of Breakdown Phenomena in MOSFET's", Proc.NASECODE II Conf. (1981) 270-274.

[76] Schütz A., Selberherr S., Pötzl H.W., "A Two-Dimensional Model of the Avalanche Effect in MOS Transistors", Solid-State Electron., **25** (1982) 177-183.

[77] Schütz A., Selberherr S., Pötzl H.W., "Analysis of Breakdown Phenomena in MOSFET's", IEEE Trans.CAD of Integrated Circuits and Systems, **CAD-1** (1982) 77-85.

[78] Selberherr S., Fichtner W., Pötzl H.W., "MINIMOS - a Program Package to Facilitate MOS Device Design and Analysis", Proc.NASECODE I Conf. (1979) 275-279.

[79] Selberherr S., Schütz A., Pötzl H.W., "MINIMOS - a Two-Dimensional MOS Transistor Analyzer", IEEE Trans.Electron Devices, **ED-27** (1980) 1540-1550.

[80] Selberherr S., "Zweidimensionale Modellierung von MOS-Transistoren", Dissertation (Technische Universität Wien, 1981).

[81] Selberherr S., Ringhofer C., "Discretization Methods for the Semiconductor Equations", Proc.NASECODE III Conf. (1983) 31-45.

[82] Selberherr S., Schütz A., Pötzl H., "Two Dimensional MOS-Transistor Modeling", in: Process and Device Modeling for Integrated Circuit Design (Martinus Nijhoff, The Hague, 1983) 490-581.

[83] Selberherr S., "Analysis and Simulation of Semiconductor Devices", (Springer, Wien New-York, 1984).

[84] Selberherr S., Griebel W., Pötzl H., "Transport Physics for Modeling Semiconductor Devices", in: Simulation of Semiconductor Devices and Processes (Pineridge Press, Swansea, 1984) 133-152.

[85] Selberherr S., Ringhofer C., "Implications of Analytical Investigations about the Semiconductor Equations on Device Modeling Programs", IEEE Trans.CAD of Integrated Circuits and Systems, **CAD-3** (1984) 52-64.

[86] Shekhar C., Khokle W.S., "Transient Behaviour of Impact Ionization in Silicon", IEEE Trans.Electron Devices, **ED-23** (1976) 1109-1110.

[87] Shichijo H., Hess K., "Band Structure Dependent Transport and Impact Ionization in GaAs", Physical Review B, **23** (1981) 4197-4207.

[88] Shichijo H., Hess K., Stillman G.E., "Simulation of High-Field Transport in GaAs Using a Monte Carlo Method and Pseudopotential Band Structures", Appl.Phys.Lett., **38** (1981) 89-91.

[89] Shigyo N., Konaka M., Dang R.L.M., "Three-Dimensional Simulation of Inverse Narrow-Channel Effect", Electron.Lett., **18** (1982) 274-275.

[90] Shockley W., "Problems Related to p-n Junctions in Silicon", Solid-State Electron., **2** (1961) 35-67.

[91] Spirito P., "Avalanche Multiplication Factors in Ge and Si Abrupt Junctions", IEEE Trans.Electron Devices, **ED-21** (1974) 226-231.

[92] Sun S.C., Plummer J.D., "Electron Mobility in Inversion and Accumulation Layers on Thermally Oxidized Silicon Surfaces", IEEE Trans.Electron Devices, **ED-27** (1980) 1497-1508.

[93] Sunami H., Shimohigashi K., Hashimoto N., "Characteristics of a Buried-Channel Graded Drain with Punchthrough Stopper (BGP) MOS Device", IEEE Trans.Electron Devices, **ED-29** (1982) 607-610.

[94] Sutherland A.D., "An Improved Empirical Fit to Baraff's Universal Curves for the Ionization Coefficients of Electron and Hole Multiplication in Semiconductors", IEEE Trans.Electron Devices, **ED-27** (1980) 1299-1300.

[95] Sze S.M., Gibbons G., "Avalanche Breakdown Voltages of Abrupt and Linearly Graded p-n Junctions in Ge, Si, GaAs, and GaP", Appl.Phys.Lett., **8** (1966) 111-113.

[96] Sze S.M., "Physics of Semiconductor Devices", (Wiley, New York, 1969).

[97] Takeda E., Kume H., Toyabe T., Asai S., "Submicrometer MOSFET Structure for Minimizing Hot-Carrier Generation", IEEE Trans.Electron Devices, **ED-29** (1982) 611-618.

[98] Tam S., Ko P.K., Hu C., "Lucky-Electron Model of Channel Hot-Electron Injection in MOSFET's", IEEE Trans.Electron Devices, **ED-31** (1984) 1116-1125.

[99] Tamer A.A., Rauch K., Moll J.L., "Numerical Comparison of DMOS, VMOS and UMOS Power Transistors", IEEE Trans.Electron Devices, **ED-30** (1983) 73-76.

[100] Tang J.Y., Shichijo H., Hess K., Iafrate G.J., "Band Structure Dependent Impact Ionization in Silicon and Gallium Arsenide", Journal de Physique, **C7** (1981) 63-69.

[101] Temple V.A.K., Adler M.S., "Calculation of the Diffusion Curvature Related Avalanche Breakdown in High-Voltage Planar p-n Junctions", IEEE Trans.Electron Devices, **ED-22** (1975) 910-916.

[102] Thornber K.K., "Relation of Drift Velocity to Low-Field Mobility and High-Field Saturation Velocity", J.Appl.Phys., **51** (1980) 2127-2136.

[103] Thornber K.K., "Applications of Scaling to Problems in High-Field Electronic Transport", J.Appl.Phys., **52** (1981) 279-290.

[104] Tihanyi J., "A Qualitative Study of the DC Performance of SIPMOS Transistors", SIEMENS For, **9** (1980) 181-189.

[105] Tihanyi J., "Integrated Power Devices", Proc.IEDM (1982) 6-10.

[106] Toyabe T., Yamaguchi K., Asai S., Mock M.S., "A Numerical Model of Avalanche Breakdown in MOSFET's", IEEE Trans.Electron Devices, **ED-25** (1978) 825-832.

[107] Toyabe T., Asai S., Yamaguchi K., "Internal Documents on the CADDET Program", (Hitachi, Tokyo, 1979).

[108] Toyabe T., Yamaguchi K., Asai S., Mock M.S., "A Two-Dimensional Avalanche Breakdown Model of Submicron MOSFET's", Proc.IEDM (1980) 432-435.

[109] VanDeWiele F., Engl W.L., Jespers P.G., "Process and Device Modeling for Integrated Circuit Design", (Noordhoff, Leyden, 1977).

[110] VanOverstraeten R., DeMan H., "Measurement of the Ionization Rates in Diffused Silicon p-n Junctions", Solid-State Electron., **13** (pp.1970) 583-608.

[111] Vandorpe D., Xuong N.H., "Mathematical 2-Dimensional Model of Semicondcutor Devices", Electron.Lett., **7** (1971) 47-50.

[112] Vandorpe D., Borel J., Merckel G., Saintot P, "An Accurate Two-Dimensional Numerical Analysis of the MOS Transistor", Solid-State Electron., **15** (1972) 547-557.

[113] Vasil'eva A.B., Stel'makh V.G., "Singularly Disturbed Systems of the Theory of Semiconductor Devices", Math.Fiz., **17** (1977) 339-348.

[114] Vasil'eva A.B., Butuzov V.F., "Singularly Perturbed Equations in the Critical Case", translated Report 2039 (MRC, University of Wisconsin, 1978).

[115] Vass E., Hess K., "Energy Loss of Warm and Hot Carriers in Surface Inversion Layers of Polar Semiconductors", Z.Physik, **B25** (1976) 323-325.

[116] Watanabe D.S., Slamet S., "Numerical Simulation of Hot-Electron Phenomena", IEEE Trans.Electron Devices, **ED-30** (19833) 1042-1049.

[117] Wilson C.L., Blue J.L., "Two-Dimensional Finite Element Charge-Sheet Model of a Short Channel MOS Transistor", Solid-State Electron., **25** (1982) 461-477.

[118] Wolff P.A., "Theory of Multiplication in Silicon and Germanium", Physical Review, **95** (1954) 1415-1420.

[119] Yamaguchi K., "Field-Dependant Mobility Model for Two-Dimensional Numerical Analysis of MOSFET's", IEEE Trans.Electron Devices, **ED-26** (1979) 1068-1074.

[120] Yamaguchi K., Takahashi S., "Theoretical Characterization and High-Speed Performance Evaluation of GaAs IGFET's", IEEE Trans.Electron Devices, **ED-28** (1981) 581-587.

[121] Yamaguchi K., "A Mobility Model for Carriers in the MOS Inversion Layer", IEEE Trans.Electron Devices, **ED-30** (1983) 658-663.

[122] Yamaguchi K., "A Time Dependent and Two Dimensional Numerical Model for MOSFET Device Operation", Solid-State Electron., **26** (1983) 907-916.